

# MoE-CAP: Benchmarking Cost, Accuracy and Performance of Sparse Mixture-of-Experts Systems

Yao Fu <sup>\*1</sup> Yinsicheng Jiang <sup>\*1</sup> Yeqi Huang <sup>\*1</sup> Ping Nie <sup>2</sup> Zhan Lu <sup>1</sup> Leyang Xue <sup>1</sup> Congjie He <sup>1</sup> Man-Kit Sit <sup>1</sup>  
 Jilong Xue <sup>3</sup> Li Dong <sup>3</sup> Ziming Miao <sup>3</sup> Kai Zou <sup>4</sup> Edoardo Ponti <sup>1,5</sup> Luo Mai <sup>1</sup>

## Abstract

The Mixture-of-Experts (MoE) architecture is increasingly favored for scaling Large Language Models (LLMs). Its key feature, sparse activation, selectively activates only a subset of parameters (experts) per token, reducing memory bandwidth and compute FLOPS compared to dense models. To capitalize on this, MoE designers leverage heterogeneous compute and memory hardware to lower system costs. However, the interaction between model sparsity and hardware heterogeneity introduces trade-offs in Cost, Accuracy, and Performance (CAP). To address this, we introduce MoE-CAP, a benchmarking method for evaluating sparse MoE systems across these three dimensions. Its key innovation is a sparsity-aware CAP analysis model, the first to integrate cost, performance, and accuracy metrics into a single diagram while estimating the impact of sparsity on system performance. MoE-CAP helps practitioners optimize hardware provisioning for an MoE model—or vice versa. MoE-CAP supports various MoE models and provides more accurate metrics than existing methods.

## 1. Introduction

Recent large language models (LLMs) are increasingly adopting Mixture-of-Experts (MoE) architectures, notable examples of which include DeepSeek (DeepSeek-AI et al., 2025), Switch-C (Fedus et al., 2022), DBRX, Mixtral-8x22B (Jiang et al., 2024), Snowflake Arctic (Snowflake AI Research, 2024), XAI Grok (XAI, 2024), and Qwen-MoE (Bai et al., 2023). These models utilize sparse experts grouped into an MoE layer, and these experts are selectively activated through a router (or a gating network). By routing tokens to a subset of experts, MoEs achieve sub-linear

computational costs compared to their dense equivalents, allowing for the building of trillion-parameter-scale LLMs.

Current MoE systems are becoming complex due to three main factors: (i) the growing sophistication of MoE layers and gating networks (or routers), which exhibit varying sparsity characteristics across models—sparsity being the ratio of activated to total parameters per token; (ii) the increasing deployment of MoE systems across different scenarios (e.g., online/offline inference, post-training), each with distinct hardware constraints, batch sizes, and service-level objective (SLO) settings; and (iii) the sub-linear computational complexity of MoEs, enabling less frequently activated experts to offload to heterogeneous processors (e.g., CPUs). This reduces reliance on costly High Bandwidth Memory (HBM) and GPU compute substantially, as demonstrated by recent efforts to run a full MoE model (DeepSeek-R1) using CPU-side host memory and matrix/vector computing (e.g., Intel AMX, ARM SME).

To manage this complexity, MoE practitioners seek methods to benchmark cost, accuracy (in downstream tasks), and performance (time and memory efficiency) for optimized deployment. However, benchmarking is challenging due to the following reasons. (i) *Poor understanding of cost–accuracy–performance trade-offs*: While MoE systems claim benefits in all three aspects, real-world deployments often reveal underestimated costs, unfulfilled performance gains, and compromised accuracy. Clear evaluation principles are needed to assess their interplay. (ii) *Inadequate system performance metrics*: Existing metrics like Memory Bandwidth Utilization (MBU; Agarwal et al., 2023) and Model FLOPS Utilization (MFU; Chowdhery et al., 2023) overlook MoE models’ sparse activation patterns, leading to overestimated memory and compute costs and inefficient GPU resource allocation. (iii) *Incomplete cost estimation across deployment scenarios*: Current benchmarks focus on GPU usage and pre-training, neglecting emerging use cases like post-training and inference, which involve varying service-level objectives, batch sizes, and diverse hardware (e.g., personal machines, cloud servers). Ignoring these factors results in inaccurate cost estimations.

To address these challenges, this paper introduces MoE-

<sup>\*</sup>Equal contribution <sup>1</sup>University of Edinburgh <sup>2</sup>LightSpeed Studio, Tencent <sup>3</sup>Microsoft Research <sup>4</sup>NetMind.AI <sup>5</sup>NVIDIA. Correspondence to: Luo Mai <luo.mai@ed.ac.uk>.

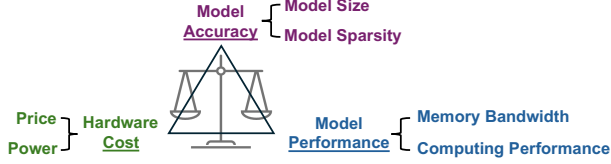


Figure 1. MoE-CAP elucidates the trade-offs among model accuracy, hardware cost, and model performance in MoE systems.

CAP, a new benchmark for evaluating the cost, accuracy, and performance (CAP) of MoE systems. As shown in Figure 1, MoE-CAP analyzes trade-offs among hardware cost, model performance, and model accuracy. Specifically, costs are assessed by hardware price and power consumption. Accuracy is dependent on MoE model size and sparsity configuration (i.e., the ratio of activated parameters per token). Performance is measured by memory bandwidth or compute demands (e.g., OPS or FLOPS).

Our benchmark reveals how MoE system designers navigate trade-offs, typically optimizing two of the three factors—cost, performance, and accuracy—while compromising the third. For example, offloading-enabled systems prioritize accuracy and cost at the expense of performance, whereas GPU-based systems with full HBM maximize accuracy and performance but incur high costs.

To quantify these trade-offs, we introduce sparsity-aware CAP analysis, featuring the first benchmarking diagram that can quantify and visualize cost, accuracy, and performance in a single view. To provide even more refined estimates within the benchmark, we propose Sparsity-aware MBU (S-MBU) and Sparsity-aware MFU (S-MFU), which account for MoE model sparsity and provide a precise measure of its impact on system performance, accuracy, and cost.

MoE-CAP provides key insights into MoE systems and AI hardware. A notable example is how the recent open-source MoE model DeepSeek-R1, which sparked a global discussion, is influencing AI infrastructure investments. Results, visualized in Figure 2, plot peak bandwidth against power consumption, comparing processor capabilities from edge devices to data centers. Each MoE model is represented by two horizontal lines: one for its activation at batch size 1 and another for full activation as batch size increases. For example, a fully activated DeepSeek-R1 requires 13,719 GB/s, achievable only with costly data center systems like the DGX-H100 (10,200W). In contrast, at batch size 1—typical for single-user inference on personal machines—the requirement drops to 1,040 GB/s, manageable by consumer-grade accelerators like the RTX 4090 (450W). These results explain financial market concerns that MoE models may reduce demand for power-hungry data center systems while enabling widespread deployment on personal machines.

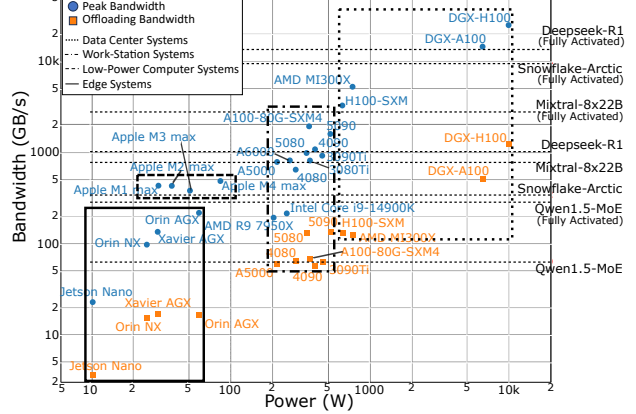


Figure 2. Highlight of MoE system benchmarking: Memory bandwidth versus Power for AI devices. Horizontal lines indicate the minimum bandwidth required for MoE models to meet a specified decoding latency. Each model is evaluated under two scenarios: fully activated (large batch size) and minimum activated (batch size = 1). Blue dots represent peak memory bandwidth and TDP, while orange dots indicate bandwidth and TDP when offloading to DRAM is needed. Systems with dots above the horizontal line meet the latency requirement, while those below do not. Systems are clustered based on their target applications, such as edge systems (autonomous driving, robotics), low-power computers, workstations, and data centers.

## 2. Background and Motivation

We summarize the key properties of popular MoE models in Table 1. These models typically have massive parameter counts, with some reaching 1.57 trillion. However, only a subset (1–28%) is activated per token. MoE models exhibit diverse sparsity characteristics; for example, Mistral-8x22B features large experts (0.3 billion parameters each) but limits the number of experts per layer to 8. In contrast, Snowflake Arctic uses 128 experts per layer, though each expert is smaller (0.1 billion parameters). This complexity extends to router design, which typically selects the top-K experts (K ranging from 1 to 8) for activation. Some architectures further introduce hybrid designs, combining perpetually active “shared” experts with conditionally activated subsets, adding another axis of variation.

**Growing system design space and complexity.** MoE systems exhibit sub-linear computational complexity but still require increasing memory resources to accommodate all potentially activated experts. In order to enhance memory efficiency, the following system designs have recently emerged to address these challenges: (i) Quantization-based designs, including unified quantization for all experts (e.g., GPTQ (Frantar et al., 2022), AWQ (Lin et al., 2023), SmoothQuant (Xiao et al., 2023)) and expert-specific adaptive quantization (e.g., QMoE (Frantar & Alistarh, 2023), MoQE (Kim et al., 2023)). (ii) Offloading-based

Table 1. Sparsity properties of popular open-source MoE models.

| Model             | Total Param | Active Param | Experts | Top-k + Shared |
|-------------------|-------------|--------------|---------|----------------|
| Switch-C          | 1571B       | 12B          | 128     | 1              |
| DBRX              | 132B        | 36B          | 16      | 4              |
| Mistral-8x22B     | 141B        | 39B          | 8       | 2              |
| Snowflake Arctic  | 480B        | 17B          | 128     | 2              |
| Grok-1            | 314B        | 77B          | 8       | 2              |
| DeepSeek-R1       | 671B        | 37B          | 256     | 8 + 1          |
| Qwen1.5-MoE       | 14.3B       | 2.7B         | 60      | 4 + 4          |
| Moonlight-16B-A3B | 16B         | 3B           | 64      | 6 + 2          |

designs, such as MoE-layer-wise parameter offloading (e.g., DeepSpeed-Inference (Aminabadi et al., 2022), SwapAdvisor (Huang et al., 2020)) and fine-grained expert-level offloading (e.g., MoE-Infinity (Xue et al., 2024), Brainstorm (Cui et al., 2023), Mixtral-Offloading (Eliseev & Mazur, 2023)). (iii) CPU-assisted computation, where less compute-intensive experts are processed on CPUs to offload work from GPUs (e.g., Fiddler (Kamahori et al., 2024)).

**Increasing use of heterogeneous hardware.** The inherent sparsity of MoE architectures has led system designers to increasingly utilize heterogeneous resources for hosting sparse experts, optimizing cost-performance trade-offs. These resources are typically more cost-effective than GPUs while still providing sufficient computing performance and memory bandwidth for certain MoE operations. They include: (i) Heterogeneous compute resources, such as CPUs integrated within GPUs (e.g., Grace-Hopper ARM chips) and external CPUs (e.g., AMD and Intel x86 chips). (ii) Heterogeneous memory resources, including LPDDR and HBM in Grace-Hopper Superchips, DRAM in host CPUs, and high-speed SSDs. (iii) Heterogeneous communication resources, such as chip-to-chip links for HBM-DRAM within GPUs, PCIe for external GPU communication, and NVLink for inter-GPU transfers.

**Strong demands for evaluating application performance, hardware cost, and model accuracy.** Given the complexity and high cost of deploying MoE systems, users must comprehensively evaluate them to determine the most cost-effective model and resource configuration. This evaluation typically relies on benchmarks that measure: (i) *application performance*, including memory bandwidth and computing performance demands, depending on the bottlenecks of target scenarios (e.g., inference or fine-tuning); (ii) *hardware cost*, considering price and power consumption for the chosen hardware; and (iii) *model accuracy*, assessed through metrics such as downstream task accuracy, language modeling perplexity, and hallucination rates.

### 3. Existing Systems and Benchmarks

#### 3.1. Analyzing Existing MoE Systems through CAP

We survey numerous existing MoE approaches in terms of application performance, hardware cost, and model accuracy. We observe that most, if not all, of these MoE systems optimize for two of these objectives while compromising the third. They can be categorized as follows:

**MoE systems for Performance and Accuracy.** Improving performance while maintaining accuracy can be achieved through two primary approaches: (i) scaling up device memory by utilizing high-end GPUs with large memory (e.g., H200 NVL with 141 GB, MI300X with 192 GB), and (ii) scaling out memory via parallel and distributed computing, leveraging technologies such as NVLink, NVSwitch, and InfiniBand, along with techniques like Tensor, Pipeline, and Expert parallelism (Li et al., 2023a; Holmes et al., 2024; Li et al., 2023b; Kwon et al., 2023; NVIDIA, 2023). However, these approaches have notable drawbacks: the exponential rise in system costs due to the increasing complexity of high-speed memory manufacturing and the sub-linear scaling efficiency of distributed systems, where communication overhead becomes a bottleneck at larger scales.

**MoE systems for Performance and Cost.** To enhance system performance without increasing costs, MoE models can adopt (i) quantization as low as 8bit (Dettmers et al., 2022; Yi et al., 2023), 4bit (Frantar et al., 2022; Lin et al., 2023; Tang et al., 2024) or even 1bit (Ma et al., 2024) or (ii) compression, such as model distillation (Hsieh et al., 2023) and sparsification (Anselli et al., 2024; Nawrot et al., 2024; Zhong et al., 2024). These methods reduce computational and memory demands but lead to inevitable performance degradation, particularly in terms of accuracy.

**MoE systems for Cost and Accuracy.** In constrained hardware environments, some systems aim to maintain model accuracy within a limited budget (e.g., relying on low-end GPUs or a restricted number of GPUs). Techniques such as memory swapping (Xue et al., 2024; Cao et al., 2024) are employed to offload model parameters or KV caches based on sparsity. Additionally, some systems utilize CPUs to assist GPU operations during model inference or generation (Kamahori et al., 2024). These systems, however, still introduce performance degradation.

#### 3.2. Limitations of Existing Benchmarks

MoE systems are often benchmarked using standard LLM evaluation methods, which overlook the impact of sparsity on cost, performance, and accuracy. Existing benchmarks, including MLPerf (Reddi et al., 2020), ML-Energy (You et al., 2023), Open-LLM-Leaderboard (Beeching et al., 2023), LLM-Perf (Ilyas Moutawwakil, 2023), Tensor-

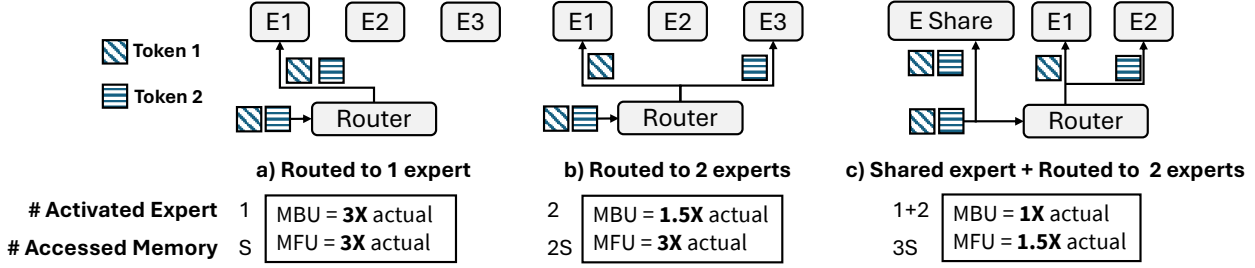


Figure 3. MoE model memory access and performance metrics under three routing scenarios.  $S$  represents the size of a single expert. The existing definitions of MBU or MFU include the cost of every expert, without taking routing or expert selection mechanisms into consideration. We indicate how much MBU/MFU is overestimated as a result, compared to the actual MBU/MFU.

Dock (TensorDock, 2024), and Artificial Analysis (Artificial Analysis, 2024), primarily assess LLMs using three types of metrics: (i) overall application performance, such as token throughput, prefill time, and decoding time; (ii) cost metrics focused solely on GPU usage; and (iii) low-level hardware metrics like MBU and MFU to identify memory and compute bottlenecks (Agarwal et al., 2023).

LLM-Viewer (Yuan et al., 2024), for example, visualizes a roofline model to analyze performance limits across different hardware based on theoretical resource requirements. However, when these benchmarks are applied to MoE systems, they reveal several limitations.

**(1) Lack of principles to understand the trade-off in MoE systems.** MoE systems claim advantages in cost, accuracy, and performance, but real-world deployments often expose challenges. Costs are frequently underestimated, performance gains over dense models fall short, and accuracy is compromised. Clear principles are needed to help users assess and navigate these trade-offs effectively.

**(2) Inaccurate system performance analysis metrics.** The commonly used MBU (Agarwal et al., 2023) and MFU (Chowdhery et al., 2023) metrics fail to consider the selective activation within sparse MoE layers. MBU measures memory bandwidth utilization as  $MBU = \frac{B_{achieved}}{B_{peak}} = \frac{(S_{model} + S_{KV})/TPOT}{B_{peak}}$ , where  $S_{model}$  represents the full model size and  $S_{KV}$  is the KV cache size. Similarly, MFU measures compute utilization as  $MFU = (T_{token} \times F_{token}) / F_{peak}$ , assuming all parameters participate in computation. However, as illustrated in Figure 3, these metrics significantly overestimate resource utilization by assuming all experts are active, especially when batch size  $> 1$ . For example, when only one expert out of three is activated (case a), both MBU and MFU are inflated by 3x. Even with shared experts (case c), the metrics still overestimate utilization by 1.5x. This often leads operators to substantially over-provision GPUs, causing significant resource waste.

**(3) Inadequate insights to guide further optimization.** A

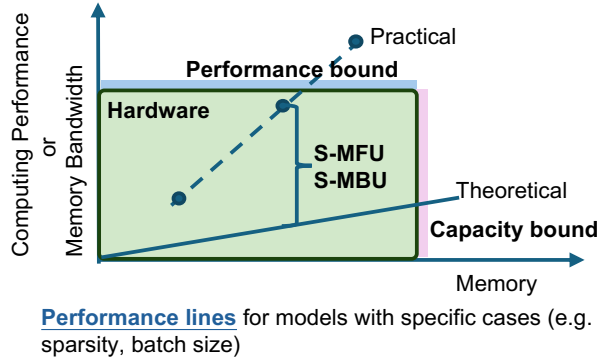


Figure 4. MoE-CAP introduces a sparsity-aware CAP analysis method that visualizes these trade-offs in a single figure, where accuracy corresponds to memory size, performance to computing performance or memory bandwidth, and cost to performance and capacity bounds. MoE-CAP provides both practical and theoretical estimations for MoE systems under different settings like sparsity or batch size.

key limitation of existing benchmarking methods is their lack of actionable insights for model and system designers on performance when model size varies, the gap between theoretical and actual performance, and optimization strategies. For example, LLM-Viewer (Yuan et al., 2024) helps users select hardware and identify bottlenecks using theoretical estimates of memory access and computational requirements. However, these estimates are unreliable for MoE systems, where activated parameters vary with batch size, requiring actual model profiling. Moreover, practical performance can vary widely across MoE systems, even when theoretical hardware performance remains constant, further limiting the applicability of theoretical estimates for deployment and optimization.

## 4. Sparsity-Aware CAP Analysis

In this section, we first introduce the CAP analysis model, defining a diagram to help users understand trade-offs and

make informed choices based on their needs. To accurately assess the gap between practical and theoretical performance requirements, we introduce new sparsity-aware metrics that capture the impact of different sparsity in MoE systems.

#### 4.1. CAP Analysis Model Diagram

Figure 4 provides an overview of the proposed CAP analysis model, structured as follows: **(i)** The x-axis represents memory capacity, which correlates with model size and directly impacts model *accuracy*. **(ii)** The y-axis captures *performance* metrics, such as operations per second (OPS) or memory bandwidth, reflecting the computational demands on hardware **(iii)** The shaded rectangular region denotes the available hardware capabilities, referred to as the *Performance-Accuracy* (PA) box. Different hardware configurations yield varying PA boxes, leading to different hardware *costs*. **(iv)** The solid line denotes the theoretical performance requirements, representing the upper limit under ideal hardware utilization. **(v)** The dashed line illustrates the practical performance demand, which accounts for real-world inefficiencies arising from MoE’s non-linear memory access due to sparse activation.

**How to use this diagram to analyze MoE systems.** The model diagram can be interpreted as follows: **(i)** When a point along the line falls within the PA box, it indicates that the specified TPOT can be achieved by a given model (i.e., with a certain accuracy and sparsity). In this case, further scaling the model size can utilize the hardware more effectively without compromising system performance. **(ii)** If a line intersects the right boundary of the PA box, it signifies a performance bottleneck due to insufficient hardware memory capacity. In this case, users should switch to hardware with larger memory to accommodate the model effectively. **(iii)** If a line intersects the top boundary of the PA box, the limiting factor is the hardware’s memory bandwidth or computing performance. Users are advised to upgrade to hardware with greater memory bandwidth or computing performance. **(iv)** In either of the above scenarios, adjusting the model’s sparsity can help optimize the trade-off between hardware memory capacity and computing performance (or memory bandwidth). **(v)** An intersection at the top-right corner of the PA box indicates an optimal match between the model and the hardware for the given performance requirements.

To demonstrate the practical utility of MoE-CAP, Figure 5 presents a CAP analysis diagram that helps MoE system practitioners make informed trade-offs. The evaluation uses the MATH dataset with a batch size of 1 and a target latency of 12.5 ms per output token. The experiments are conducted using vLLM on a single A100-80G-PCIe (1935 GB/s peak bandwidth, 80 GB VRAM) (left) and a single A6000 (768 GB/s peak bandwidth, 48 GB VRAM) (right). We evaluate

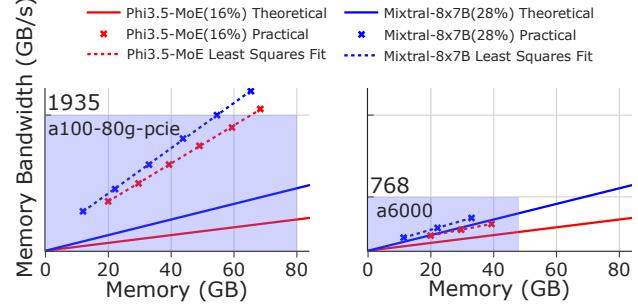


Figure 5. Illustrative CAP analysis diagrams for MoE models Mixtral-8x7B (Jiang et al., 2024) and Phi3.5-MoE (Abdin et al., 2024), with sparsity levels of 28% and 16% respectively, evaluated at a batch size of 1 and a TPOT requirement of 12.5ms per token on a single A100-80G-PCIe (left) and a single A6000 (right) using vLLM.

Mixtral-8x7B (Jiang et al., 2024) and Phi3.5-MoE (Abdin et al., 2024), with sparsity levels of 28% and 16% respectively. Different model sizes are obtained by varying the number of layers.

Figure 5 provides several key insights from our MoE-CAP analysis. First, while MoE models are often assumed to be memory capacity-bound, our S-MBU measurements reveal that on both NVIDIA A100 80GB and A6000, they are actually memory bandwidth-bound, suggesting that users should upgrade to higher-bandwidth hardware (e.g., H100) for better performance. Second, for models of Phi3.5-MoE family around 40GB, neither A100 nor A6000 is bandwidth-bound, making the A6000 a more cost-effective choice. Third, for models exceeding 60GB, the A100 fails to meet the required output latency due to bandwidth constraints, as indicated by the estimated performance point falling outside the hardware capability region. Lastly, we observe that memory bandwidth requirements scale linearly with model size, indicating that S-MBU changes regularly and is predictable within a model family. This finding is particularly valuable for model designers, as it enables performance predictions using smaller models to determine the optimal hardware for deployment.

#### 4.2. CAP Analysis Model Inputs

The proposed analysis model is driven by these inputs: **(i)** The peak bandwidth or OPS of the hardware; **(ii)** The configuration of the model, such as activated parameters per token  $p_{\text{activated}}$ , per token KV cache size  $s_{\text{kv}}$ ; **(iii)** The basic system performance requirements include required time-per-output-token TPOT<sup>r</sup> along with the batch size  $bs$  and sequence length  $l_{\text{seq}}$ ; **(iv)** The profiled S-MBU (Sparse Model Bandwidth Utilization) or S-MFU (Sparse Model FLOPs Utilization).

The theoretical performance requirements are derived from

the given inputs, assuming optimal hardware utilization. They are defined as follows:

$$\text{Theoretical Bandwidth} = \frac{S_{\text{activated}} + S_{\text{KV}}}{\text{TPOT}^r} \quad (1)$$

$$\text{Theoretical OPS} = \frac{2bs(p_{\text{activated}} + l_{\text{seq}}s_{\text{kv}})}{\text{TPOT}^r} \quad (2)$$

Here,  $S$  denotes the amount of accessed memory, with  $S_{\text{activated}}$  representing the memory required for activated parameters and  $S_{\text{KV}}$  denoting the average memory size of the KV cache per token. The term  $l_{\text{seq}}s_{\text{kv}}$  captures the required FLOPs to compute the attention score over the existing KV cache (i.e.,  $l_{\text{seq}}$  tokens), where  $s_{\text{kv}}$  is the per-token KV states size and may differ across various attention mechanisms. The constant 2 in Equation 2 reflects the assumption that each parameter undergoes two operations—one multiplication and one addition—common in matrix multiplication. We omit element-wise operations because they can be fused into matrix operations without additional memory access, and their computational cost is orders of magnitude lower than that of matrix computations.

In practice, MoE systems often suffer inefficiencies due to redundant data transfers or calculations, resulting in performance losses. Consequently, the calculated theoretical bandwidth or OPS may not meet the required application performance (e.g., throughput). To determine the practical hardware requirements for a given set of inputs, it is essential to consider hardware utilization. Thus, the practical performance requirement is defined as:

$$\text{Practical Bandwidth} = \frac{\text{Theoretical Bandwidth}}{\text{S-MBU}} \quad (3)$$

$$\text{Practical OPS} = \frac{\text{Theoretical OPS}}{\text{S-MFU}} \quad (4)$$

Here, S-MBU and S-MFU (defined in the next subsection) represent the actual hardware utilization for MoE models.

To illustrate, suppose the theoretical bandwidth requirement is 400 GB/s. If the hardware achieves only 50% bandwidth efficiency during model decoding, the practical bandwidth requirement must be doubled to 800 GB/s ( $\frac{400 \text{ GB/s}}{50\%}$ ) in order to meet the same throughput or latency needs.

### 4.3. Sparsity-Aware Performance Metrics

**Sparse model bandwidth utilization.** When designing a sparsity-aware MBU, we aim for a metric that is broadly applicable across various MoE models. The diverse sparsity patterns observed in MoE architectures are summarized in Figure 3, from which we derive key requirements for the new MBU metric.

First, the metric should capture which experts are activated for a batch of input tokens. For example, in case (a), a sparse feed-forward (FF) layer with three experts routes each token to a single top-1 expert. Here, both input tokens activate the same expert, resulting in memory access equivalent to a single expert's size. In contrast, case (b) shows two tokens activating different experts, doubling the accessed memory relative to case (a). Second, the metric must account for different routing mechanisms, such as shared experts introduced in recent MoE studies (DeepSeek-AI et al., 2025; Bai et al., 2023), illustrated in Figure 3 (c).

To meet the above requirements, we define Sparse Memory Bandwidth Utilization (S-MBU) based on the activated size of parameters  $S_{\text{activated}}$ , rather than the full model size  $S_{\text{model}}$ , as follows.

$$\begin{aligned} \text{S-MBU} &= \frac{B_{\text{achieved}}}{B_{\text{peak}}} = \frac{(S_{\text{activated}} + S_{\text{KV}})/\text{TPOT}}{B_{\text{peak}}}, \\ S_{\text{activated}} &= n_{\text{layer}} S_{\text{attn}} + \sum_{l=1}^{n_{\text{layer}}} \sum_{i=1}^{n_{\text{expert}}} \mathbb{1}[l, i] \times S_{\text{expert}} \end{aligned} \quad (5)$$

where  $\mathbb{1}[l, i]$  is a boolean variable indicates whether the expert indexed  $i$  at layer  $l$  is activated for computation. This ensures that only the activated parameters contribute to the accessed memory.  $\mathbb{1}[l, i]$  can be achieved by tracing router outputs.

Besides, dense models are a special case of equation (5) with  $n_{\text{expert}} = 1$  and  $\forall i, \mathbb{1}[l, i] = 1$ . Therefore, our definition is also suitable for model architectures where not all layers are MoE layers, e.g., in Switch Transformers (Fedus et al., 2022).

**Sparse model FLOPS utilization.** We aim to account for the fact that experts are sparsely activated when calculating  $F_{\text{token}}$ , i.e. FLOPs per token. Specifically, in each MoE layer, we account for top-k activated experts with shared experts, denoted  $k_{\text{expert}}$ , which can be obtained from the model configuration without the need for runtime tracing. Besides, we also account for the router component in each MoE layer,  $N_{\text{router}}$ . The attention layer remains the same. Consequently, we refine the FLOPs per token calculation as follows:

$$\text{S-MFU} = (T_{\text{token}} \times \text{S-}F_{\text{token}}) / F_{\text{peak}} \quad (6)$$

$$\text{S-}F_{\text{token}} = F_{\text{attn}} + 2 \times (N_{\text{router}} + k_{\text{expert}} N_{\text{expert}}) \quad (7)$$

where  $F_{\text{attn}}$  means FLOPs needed for attention and  $N_{\text{expert}}$  represents the number of parameters in the expert module.

### 4.4. Benchmark Implementation

We have developed MoE-CAP as a software tool that automatically collects sparsity metrics for a given MoE model and visualizes the CAP diagram, helping users efficiently

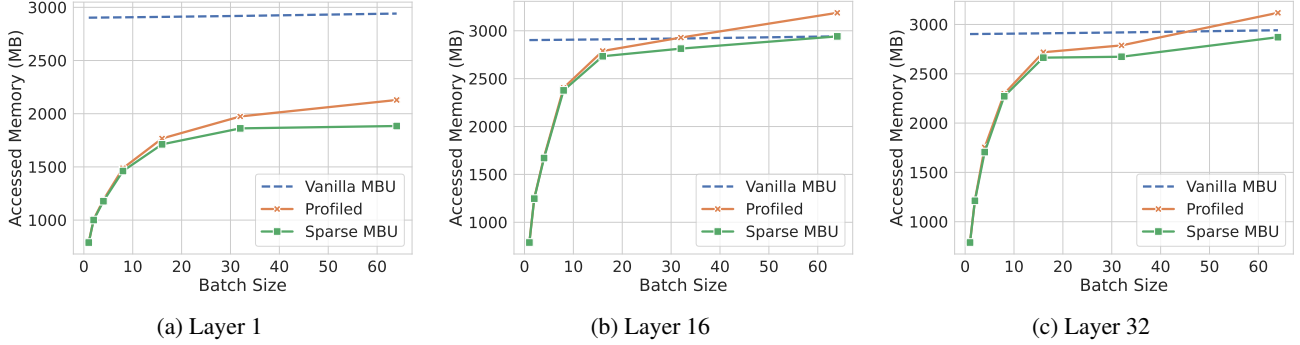


Figure 6. Correctness evaluation of the vanilla MBU, our S-MBU and actual MBU (through profiling).

analyze trade-offs. We made the process of downloading datasets and models and triggering MoE-CAP for evaluation fully automatic. The entire software is compatible with HuggingFace software, making it easy to use it as a library (e.g., importing the S-MBU and S-MFU metrics for assessing a custom MoE system). So far, we have included three popular MoE-supported LLM inference frameworks, namely `huggingface transformers` (Wolf et al., 2020), `vLLM` (Kwon et al., 2023) and `llama.cpp` (Gerganov, 2023).

## 5. Metric Evaluation and Analysis Results

This section assesses the proposed metrics and the CAP analysis model. (i) we demonstrate that the S-MBU provides a more accurate representation of the actual profiled accessed memory compared to the vanilla MBU. (ii) We then illustrate the effectiveness of our CAP analysis across different scenarios, such as single hardware setups or parallelism on multiple hardware systems, guiding users in selecting the most suitable hardware for their needs.

### 5.1. S-MBU Evaluation

We verify the proposed S-MBU with Mixtral-8x7B model. As discussed in §4, vanilla MBU is not aware of the sparse memory access. In Figure 6, we show the averaged accessed memory of a specific Transformer layer of Mixtral-8x7B model using the GSM8K dataset. We vary the input batch size from 1 to 64. With a batch size of 1, in each layer, only the top 2 experts are accessed (*i.e.* activated); instead, with increased batch sizes, more experts are accessed. However, the number of total activated experts does not necessarily increase linearly with batch size because tokens can share experts.

According to Figure 6, the vanilla MBU fails to account for the selective activation of experts in an MoE layer, resulting in an overestimation of total accessed memory by over 260%. In contrast, S-MBU captures the activated experts accurately, with less than a 1% discrepancy from the actual

memory usage profiled (based on HuggingFace Transformers). As batch size increases, we observe varying expert activation patterns across layers. For instance, with a batch size of 64, only about half of the experts are activated in the first layer, while in deeper layers like 16 and 32, nearly all experts are activated. The sparse estimation also accurately reflects the trend of increasing memory access with larger batch sizes. However, there remains a gap between the profiled results and both MBU and S-MBU when almost all experts are activated, primarily because both methods overlook the intermediate states (e.g., hidden states) that increase linearly with batch size.

### 5.2. Bandwidth-Memory Analysis

We demonstrate how to leverage the CAP model to analyze inference bandwidth and memory capacity requirements. To evaluate two models, DeepSeek-V2-Lite (DeepSeek-AI, 2024) and Qwen1.5-MoE (Bai et al., 2023), across multiple batch sizes (1, 32, 64, 128), we utilize vLLM (Kwon et al., 2023), a state-of-the-art inference engine, as the backend and conduct experiments on the MATH dataset (Hendrycks et al., 2021). Additionally, we extend the input context length to 4000 tokens to emphasize the effect of KV cache size on bandwidth requirements.

Our analysis is performed under a TPOT requirement of 250ms, using both a single A100-80G-SXM4 (2037 GB/s peak memory bandwidth, 80GB VRAM) and a single A6000 (768 GB/s peak memory bandwidth, 48GB VRAM).

Figure 7 presents the results. As the batch size increases, more parameters are activated, leading to higher bandwidth requirements. Across both models, on A6000, the system becomes bandwidth-bound when the batch size increases from 32 to 64. When the batch size is 32 or lower, our analysis indicates that neither the A6000 nor the A100 experiences bandwidth bottlenecks, allowing users to opt for the more cost-effective A6000 GPUs. Our model also reports accurate results. For instance, when the batch size is 64, the points for both models are outside the box of A6000

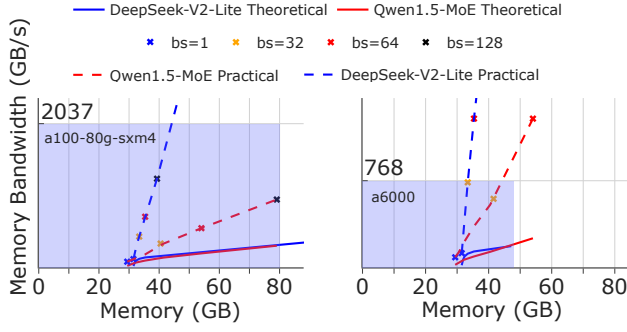


Figure 7. A Bandwidth-Memory analysis was conducted on an A100-80G-SXM4 and an A6000, targeting a TPOP of 250ms. The study evaluated performance across varying batch sizes (1, 32, 64 and 128) for both the DeepSeek-V2-Lite and Qwen1.5-MoE models.

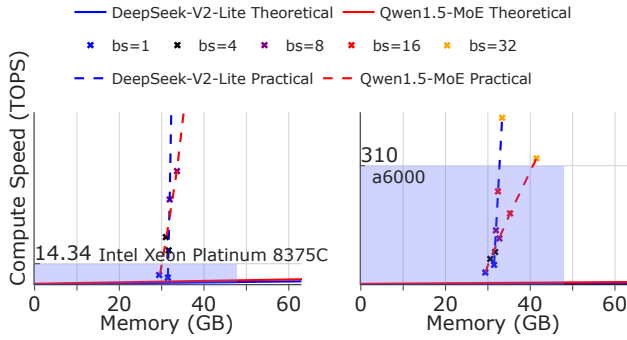


Figure 8. A Computation-Memory analysis was conducted on an Intel(R) Xeon(R) Platinum 8375C CPU and an A6000, targeting a TPOT of 250ms. The study evaluated performance across varying batch sizes (1, 4, 8, 16, and 32) for both the DeepSeek-V2-Lite and Qwen1.5-MoE models.

which suggests that neither model can achieve the 250ms per token target. This is consistent with actual performance, where they reach only 478.5ms and 486.7ms per token, respectively.

### 5.3. Computation-Memory Analysis

This analysis follows the same setup as in § 5.2, except for the batch sizes, which are set to 1, 4, 8, 16, and 32. We evaluate computational limits across two distinct hardware platforms: CPU and GPU. Specifically, we assess an Intel(R) Xeon(R) Platinum 8375C CPU (14.34 TOPS peak computing power, 48GB DDR4 DRAM) and an A6000 GPU, using the llama.cpp framework (Gerganov, 2023).

Figure 8 shows our computation-memory diagram. At batch size 1, the CPU meets performance requirements, making it suitable for personal deployment under this TPOT requirement, where batch size is typically 1. However, both models rapidly hit the computation bound as batch size increases

due to limited processing power and suboptimal matrix multiplication optimization. On the GPU, neither model encounters a performance bottleneck for batch sizes up to 16. As the batch size increases from 16 to 32, both models on the A6000 reach their computational limits, indicating that hardware with higher computing power, such as the A100, would be a more suitable choice. For DeepSeek-V2-Lite model, computational limits soon become the bottleneck with relatively smaller batch size due to its Multihead-Latent Attention mechanism that compresses the KV cache to reduce memory transfers but, in turn, increases computational demands due to the up scaling of the compressed KV cache.

Moreover, Our model accurately captures the correct performance bound. At a batch size of 32 on the A6000, neither model reaches a bandwidth limitation; however, the SLO is not met, with performance at 271.7ms and 255.3ms per token respectively. As shown in the right figure of Figure 8, this is due to hitting the computational limit, which explains the failure to achieve the SLO.

## 6. Insights and Takeaway Messages

Through MoE-CAP, we derive key insights that highlight both the potential and challenges of MoE systems:

**MoE systems enable a broader range of devices to perform inference.** Personal machines typically operate in single-user inference environments, where experts are sparsely activated with a small batch size (usually as 1). In this case, many low-power hardware platforms can run large MoE models (with the support of offloading) or smaller versions of MoE models (such as Moonlight-16B) with reasonable latency and performance. This challenges the conventional belief that large MoE models must run on expensive data center systems, as demonstrated in Figure 2.

**Hybrid computing will become more prevalent.** With emerging matrix acceleration capabilities in processors (e.g., Intel AMX, ARM SME), these processors can significantly assist GPUs in serving MoE models. They also offer greater memory flexibility, making them attractive for MoE deployment. For instance, DRAM on personal workstations can be scaled to TB levels, whereas consumer-grade GPUs are limited to 48GB. As a result, hybrid architectures combining CPUs, CPU-side memory, and GPUs will become increasingly common, especially in personal environments where small batches are prevailing.

**MoE systems should be co-designed to align with specific applications and deployment scenarios.** We observe that the sparsity characteristics of MoE models are significantly affected by the applications (e.g., online inference, offline inference, fine-tuning and pre-training) and deployment scenarios (e.g., single-user vs. multi-user, small vs.

large batch sizes). These characteristics determine system bottlenecks, which can be addressed by various hardware platforms—some offering significantly lower costs than conventional GPU-only solutions. We anticipate a surge in specialized MoE systems tailored to specific applications and scenarios.

**New benchmarking and design principles are needed for emerging sparse AI systems.** Sparsity is not unique to MoE—it also plays a critical role in emerging sparse AI systems, such as those involving sparse KV-cache architectures (common in long-context reasoning) and module-based agentic LLM workflows. In these cases, sparsity directly influences system bottlenecks, highlighting the need for new system benchmark, profiling and design principles that inherently account for cost, performance, and accuracy. With these principles, a wide range of sparsity-aware system optimizations can be unlocked. Without them, sparse AI systems risk falling short of their cost-saving potential and performance goals.

## 7. Conclusion

This paper introduces MoE-CAP, a novel and timely benchmark for understanding and evaluating emerging MoE systems. We anticipate that the proposed sparsity-aware performance metrics and CAP analysis will be crucial for accurately assessing MoE systems and guiding further improvements in their efficiency. Ultimately, MoE-CAP aims to facilitate MoE deployment across diverse AI hardware, ranging from personal machines to cloud data centers, enabling cost savings while maintaining high accuracy and system performance.

## References

Abdin, M., Aneja, J., Awadalla, H., Awadallah, A., Awan, A. A., Bach, N., Bahree, A., Bakhtiari, A., Bao, J., Behl, H., Benhaim, A., Bilenko, M., Bjorck, J., Bubeck, S., Cai, M., Cai, Q., Chaudhary, V., Chen, D., Chen, D., Chen, W., Chen, Y.-C., Chen, Y.-L., Cheng, H., Chopra, P., Dai, X., Dixon, M., Eldan, R., Fragoso, V., Gao, J., Gao, M., Gao, M., Garg, A., Giorno, A. D., Goswami, A., Gunasekar, S., Haider, E., Hao, J., Hewett, R. J., Hu, W., Huynh, J., Iter, D., Jacobs, S. A., Javaheripi, M., Jin, X., Karampatziakis, N., Kauffmann, P., Khademi, M., Kim, D., Kim, Y. J., Kurilenko, L., Lee, J. R., Lee, Y. T., Li, Y., Li, Y., Liang, C., Liden, L., Lin, X., Lin, Z., Liu, C., Liu, L., Liu, M., Liu, W., Liu, X., Luo, C., Madan, P., Mahmoudzadeh, A., Majercak, D., Mazzola, M., Mendes, C. C. T., Mitra, A., Modi, H., Nguyen, A., Norick, B., Patra, B., Perez-Becker, D., Portet, T., Pryzant, R., Qin, H., Radmilac, M., Ren, L., de Rosa, G., Rosset, C., Roy, S., Ruwase, O., Saarikivi, O., Saied, A., Salim, A., Santacroce, M., Shah, S., Shang, N., Sharma, H., Shen, Y., Shukla, S., Song, X., Tanaka, M., Tupini, A., Vaddamanu, P., Wang, C., Wang, G., Wang, L., Wang, S., Wang, X., Wang, Y., Ward, R., Wen, W., Witte, P., Wu, H., Wu, X., Wyatt, M., Xiao, B., Xu, C., Xu, J., Xu, W., Xue, J., Yadav, S., Yang, F., Yang, J., Yang, Y., Yang, Z., Yu, D., Yuan, L., Zhang, C., Zhang, C., Zhang, J., Zhang, L. L., Zhang, Y., Zhang, Y., Zhang, Y., and Zhou, X. Phi-3 technical report: A highly capable language model locally on your phone, 2024. URL <https://arxiv.org/abs/2404.14219>.

Agarwal, M., Qureshi, A., Sardana, N., Li, L., Quevedo, J., and Khudia, D. <https://www.databricks.com/blog/llm-inference-performance-engineering-best-practices> 2023.

Aminabadi, R. Y., Rajbhandari, S., Awan, A. A., Li, C., Li, D., Zheng, E., Ruwase, O., Smith, S., Zhang, M., Rasley, J., and He, Y. DeepSpeed-Inference: Enabling efficient inference of transformer models at unprecedented scale. In *SC*, pp. 46:1–46:15. IEEE, 2022.

Ansell, A., Vulić, I., Sterz, H., Korhonen, A., and Ponti, E. M. Scaling sparse fine-tuning to large language models, 2024. URL <https://arxiv.org/abs/2401.16405>.

Artificial Analysis. Artificial analysis llm performance leaderboard. <https://artificialanalysis.ai/leaderboards/models>, 2024. Accessed: 2024-06-04.

Bai, J., Bai, S., Chu, Y., Cui, Z., Dang, K., Deng, X., Fan, Y., Ge, W., Han, Y., Huang, F., Hui, B., Ji, L., Li, M., Lin, J., Lin, R., Liu, D., Liu, G., Lu, C., Lu, K., Ma, J., Men, R., Ren, X., Ren, X., Tan, C., Tan, S., Tu, J., Wang, P., Wang, S., Wang, W., Wu, S., Xu, B., Xu, J., Yang, A., Yang, H., Yang, J., Yang, S., Yao, Y., Yu, B., Yuan, H., Yuan, Z., Zhang, J., Zhang, X., Zhang, Y., Zhang, Z., Zhou, C., Zhou, J., Zhou, X., and Zhu, T. Qwen technical report. *arXiv preprint arXiv:2309.16609*, 2023.

Beeching, E., Fourrier, C., Habib, N., Han, S., Lambert, N., Rajani, N., Sanseviero, O., Tunstall, L., and Wolf, T. Open llm leaderboard. [https://huggingface.co/spaces/HuggingFaceH4/open\\_llm\\_leaderboard](https://huggingface.co/spaces/HuggingFaceH4/open_llm_leaderboard), 2023.

Cao, S., Liu, S., Griggs, T., Schafhalter, P., Liu, X., Sheng, Y., Gonzalez, J. E., Zaharia, M., and Stoica, I. Moe-lightning: High-throughput moe inference on memory-constrained gpus. *arXiv preprint arXiv:2411.11217*, 2024.

Chowdhery, A., Narang, S., Devlin, J., Bosma, M., Mishra, G., Roberts, A., Barham, P., Chung, H. W., Sutton, C., Gehrmann, S., Schuh, P., Shi, K., Tsvyashchenko, S., Maynez, J., Rao, A., Barnes, P., Tay, Y., Shazeer, N., Prabhakaran, V., Reif, E., Du, N., Hutchinson, B., Pope, R., Bradbury, J., Austin, J., Isard, M., Gur-Ari, G., Yin, P., Duke, T., Levskaya, A., Ghemawat, S., Dev, S., Michalewski, H., Garcia, X., Misra, V., Robinson, K., Fedus, L., Zhou, D., Ippolito, D., Luan, D., Lim, H., Zoph, B., Spiridonov, A., Sepassi, R., Dohan, D., Agrawal, S., Omernick, M., Dai, A. M., Pillai, T. S., Pelлат, M., Lewkowycz, A., Moreira, E., Child, R., Polozov, O., Lee, K., Zhou, Z., Wang, X., Saeta, B., Diaz, M., Firat, O., Catasta, M., Wei, J., Meier-Hellstern, K., Eck, D., Dean, J., Petrov, S., and Fiedel, N. PaLM: Scaling language modeling with pathways. *J. Mach. Learn. Res.*, 24:240:1–240:113, 2023.

Cui, W., Han, Z., Ouyang, L., Wang, Y., Zheng, N., Ma, L., Yang, Y., Yang, F., Xue, J., Qiu, L., Zhou, L., Chen, Q., Tan, H., and Guo, M. Optimizing dynamic neural networks with Brainstorm. In *OSDI*, pp. 797–815. USENIX Association, 2023.

DeepSeek-AI. Deepseek-v2: A strong, economical, and efficient mixture-of-experts language model, 2024.

DeepSeek-AI, Guo, D., Yang, D., Zhang, H., Song, J., Zhang, R., Xu, R., Zhu, Q., Ma, S., Wang, P., Bi, X., Zhang, X., Yu, X., Wu, Y., Wu, Z. F., Gou, Z., Shao, Z., Li, Z., Gao, Z., Liu, A., Xue, B., Wang, B., Wu, B., Feng, B., Lu, C., Zhao, C., Deng, C., Zhang, C., Ruan, C., Dai, D., Chen, D., Ji, D., Li, E., Lin, F., Dai, F., Luo, F., Hao, G., Chen, G., Li, G., Zhang, H., Bao, H., Xu, H., Wang, H., Ding, H., Xin, H., Gao, H., Qu, H., Li, H., Guo, J., Li, J., Wang, J., Chen, J., Yuan, J., Qiu, J., Li, J., Cai, J. L., Ni, J., Liang, J., Chen, J., Dong, K., Hu, K., Gao, K., Guan, K., Huang, K., Yu, K., Wang, L., Zhang, L., Zhao, L., Wang, L., Zhang, L., Xu, L., Xia, L., Zhang, M., Zhang, M., Tang, M., Li, M., Wang, M., Li, M., Tian, N., Huang, P., Zhang, P., Wang, Q., Chen, Q., Du, Q., Ge, R., Zhang, R., Pan, R., Wang, R., Chen, R. J., Jin, R. L., Chen, R., Lu, S., Zhou, S., Chen, S., Ye, S., Wang, S., Yu, S., Zhou, S., Pan, S., Li, S. S., Zhou, S., Wu, S., Ye, S., Yun, T., Pei, T., Sun, T., Wang, T., Zeng, W., Zhao, W., Liu, W., Liang, W., Gao, W., Yu, W., Zhang, W., Xiao, W. L., An, W., Liu, X., Wang, X., Chen, X., Nie, X., Cheng, X., Liu, X., Xie, X., Liu, X., Yang, X., Li, X., Su, X., Lin, X., Li, X. Q., Jin, X., Shen, X., Chen, X., Sun, X., Wang, X., Song, X., Zhou, X., Wang, X., Shan, X., Li, Y. K., Wang, Y. Q., Wei, Y. X., Zhang, Y., Xu, Y., Li, Y., Zhao, Y., Sun, Y., Wang, Y., Yu, Y., Zhang, Y., Shi, Y., Xiong, Y., He, Y., Piao, Y., Wang, Y., Tan, Y., Ma, Y., Liu, Y., Guo, Y., Ou, Y., Wang, Y., Gong, Y., Zou, Y., He, Y., Xiong, Y., Luo, Y., You, Y., Liu, Y., Zhou, Y., Zhu, Y. X., Xu, Y., Huang, Y., Li, Y., Zheng, Y., Zhu, Y., Ma, Y., Tang, Y., Zha, Y., Yan, Y., Ren, Z. Z., Ren, Z., Sha, Z., Fu, Z., Xu, Z., Xie, Z., Zhang, Z., Hao, Z., Ma, Z., Yan, Z., Wu, Z., Gu, Z., Zhu, Z., Liu, Z., Li, Z., Xie, Z., Song, Z., Pan, Z., Huang, Z., Xu, Z., Zhang, Z., and Zhang, Z. Deepseek-r1: Incentivizing reasoning capability in llms via reinforcement learning, 2025. URL <https://arxiv.org/abs/2501.12948>.

Dettmers, T., Lewis, M., Belkada, Y., and Zettlemoyer, L. Gpt3. int8 (): 8-bit matrix multiplication for transformers at scale. *Advances in Neural Information Processing Systems*, 35:30318–30332, 2022.

Eliseev, A. and Mazur, D. Fast inference of mixture-of-experts language models with offloading, 2023.

Fedus, W., Zoph, B., and Shazeer, N. Switch Transformers: Scaling to trillion parameter models with simple and efficient sparsity. *J. Mach. Learn. Res.*, 23:120:1–120:39, 2022.

Frantar, E. and Alistarh, D. Qmoe: Practical sub-1-bit compression of trillion-parameter models, 2023.

Frantar, E., Ashkboos, S., Hoefer, T., and Alistarh, D. GPTQ: accurate post-training quantization for generative pre-trained transformers, 2022.

Gerganov, G. llama.cpp. <https://github.com/ggerganov/llama.cpp>, 2023.

Hendrycks, D., Burns, C., Kadavath, S., Arora, A., Basart, S., Tang, E., Song, D., and Steinhardt, J. Measuring mathematical problem solving with the math dataset, 2021. URL <https://arxiv.org/abs/2103.03874>.

Holmes, C., Tanaka, M., Wyatt, M., Awan, A. A., Rasley, J., Rajbhandari, S., Aminabadi, R. Y., Qin, H., Bakhtiari, A., Kurilenko, L., and He, Y. DeepSpeed-FastGen: High-throughput text generation for LLMs via MII and DeepSpeed-Inference, 2024.

Hsieh, C.-Y., Li, C.-L., Yeh, C.-K., Nakhost, H., Fujii, Y., Ratner, A., Krishna, R., Lee, C.-Y., and Pfister, T. Distilling step-by-step! outperforming larger language models with less training data and smaller model sizes. *arXiv preprint arXiv:2305.02301*, 2023.

Huang, C., Jin, G., and Li, J. SwapAdvisor: Pushing deep learning beyond the GPU memory limit via smart swapping. In *ASPLOS*, pp. 1341–1355. ACM, 2020.

Ilyas Moutawwakil, R. P. Llm-perf leaderboard. <https://huggingface.co/spaces/optimum/llm-perf-leaderboard>, 2023.

Jiang, A. Q., Sablayrolles, A., Roux, A., Mensch, A., Savary, B., Bamford, C., Chaplot, D. S., de Las Casas, D., Hanna, E. B., Bressand, F., Lengyel, G., Bour, G., Lample, G., Lavaud, L. R., Saulnier, L., Lachaux, M., Stock, P., Subramanian, S., Yang, S., Antoniak, S., Scao, T. L., Gervet, T., Lavril, T., Wang, T., Lacroix, T., and Sayed, W. E. Mixtral of experts, 2024.

Kamahori, K., Gu, Y., Zhu, K., and Kasikci, B. Fiddler: CPU-GPU orchestration for fast inference of mixture-of-experts models, 2024.

Kim, Y. J., Fahim, R., and Awadalla, H. H. Mixture of quantized experts (MoQE): Complementary effect of low-bit quantization and robustness, 2023.

Kwon, W., Li, Z., Zhuang, S., Sheng, Y., Zheng, L., Yu, C. H., Gonzalez, J., Zhang, H., and Stoica, I. Efficient memory management for large language model serving with pagedattention. In *SOSP*, pp. 611–626. ACM, 2023.

Li, J., Jiang, Y., Zhu, Y., Wang, C., and Xu, H. Accelerating distributed MoE training and inference with Lina. In *USENIX Annual Technical Conference*, pp. 945–959. USENIX Association, 2023a.

Li, Z., Zheng, L., Zhong, Y., Liu, V., Sheng, Y., Jin, X., Huang, Y., Chen, Z., Zhang, H., Gonzalez, J. E., and Stoica, I. AlpaServe: Statistical multiplexing with model parallelism for deep learning serving. In *OSDI*, pp. 663–679. USENIX Association, 2023b.

Lin, J., Tang, J., Tang, H., Yang, S., Dang, X., and Han, S. AWQ: activation-aware weight quantization for LLM compression and acceleration, 2023.

Ma, S., Wang, H., Ma, L., Wang, L., Wang, W., Huang, S., Dong, L., Wang, R., Xue, J., and Wei, F. The era of 1-bit llms: All large language models are in 1.58 bits. *arXiv preprint arXiv:2402.17764*, 2024.

Nawrot, P., Łaniczki, A., Chochowski, M., Tarjan, D., and Ponti, E. M. Dynamic memory compression: Retrofitting llms for accelerated inference, 2024. URL <https://arxiv.org/abs/2403.09636>.

NVIDIA. TensorRT-LLM. <https://github.com/NVIDIA/TensorRT-LLM>, 2023.

Reddi, V. J., Cheng, C., Kanter, D., Mattson, P., Schmuelling, G., Wu, C.-J., Anderson, B., Breughe, M., Charlebois, M., Chou, W., Chukka, R., Coleman, C., Davis, S., Deng, P., Diamos, G., Duke, J., Fick, D., Gardner, J. S., Hubara, I., Idgunji, S., Jablin, T. B., Jiao, J., John, T. S., Kanwar, P., Lee, D., Liao, J., Likhmatov, A., Massa, F., Meng, P., Micikevicius, P., Osborne, C., Pekhimenko, G., Rajan, A. T. R., Sequeira, D., Sirasao, A., Sun, F., Tang, H., Thomson, M., Wei, F., Wu, E., Xu, L., Yamada, K., Yu, B., Yuan, G., Zhong, A., Zhang, P., and Zhou, Y. Mlperf inference benchmark. In *2020 ACM/IEEE 47th Annual International Symposium on Computer Architecture (ISCA)*, pp. 446–459, 2020. doi: 10.1109/ISCA45697.2020.00045.

Snowflake AI Research. Snowflake Arctic: The best LLM for enterprise AI — efficiently intelligent, truly open. <https://www.snowflake.com/blog/arctic-open-efficient-foundation-language-models-2024>. Accessed: 2024-06-04.

Tang, P., Liu, J., Hou, X., Pu, Y., Wang, J., Heng, P.-A., Li, C., and Guo, M. Hobbit: A mixed precision expert offloading system for fast moe inference, 2024.

TensorDock. Tensordock - machine learning gpu benchmarks. <https://tensordock.com/benchmarks>, 2024. Accessed: 2024-06-04.

Wolf, T., Debut, L., Sanh, V., Chaumond, J., Delangue, C., Moi, A., Cistac, P., Rault, T., Louf, R., Funtowicz, M., Davison, J., Shleifer, S., von Platen, P., Ma, C., Jernite, Y., Plu, J., Xu, C., Scao, T. L., Gugger, S., Drame, M., Lhoest, Q., and Rush, A. M. Transformers: State-of-the-art natural language processing. In *Proceedings of the 2020 Conference on Empirical Methods in Natural Language Processing: System Demonstrations*, pp. 38–45, Online, October 2020. Association for Computational Linguistics. URL <https://www.aclweb.org/anthology/2020.emnlp-demos.6>.

XAI. Open release of Grok-1. <https://x.ai/blog/grok-os>, 2024. Accessed: 2024-06-04.

Xiao, G., Lin, J., Seznec, M., Wu, H., Demouth, J., and Han, S. SmoothQuant: Accurate and efficient post-training quantization for large language models. In *ICML*, volume 202 of *Proceedings of Machine Learning Research*, pp. 38087–38099. PMLR, 2023.

Xue, L., Fu, Y., Lu, Z., Mai, L., and Marina, M. Moe-infinity: Activation-aware expert offloading for efficient moe serving, 2024.

Yi, R., Guo, L., Wei, S., Zhou, A., Wang, S., and Xu, M. EdgeMoE: Fast on-device inference of moe-based large language models, 2023.

You, J., Chung, J.-W., and Chowdhury, M. Zeus: Understanding and optimizing GPU energy consumption of DNN training. In *USENIX NSDI*, 2023.

Yuan, Z., Shang, Y., Zhou, Y., Dong, Z., Zhou, Z., Xue, C., Wu, B., Li, Z., Gu, Q., Lee, Y. J., Yan, Y., Chen, B., Sun, G., and Keutzer, K. Llm inference unveiled: Survey and roofline model insights, 2024. URL <https://arxiv.org/abs/2402.16363>.

Zhong, S., Liang, L., Wang, Y., Wang, R., Huang, R., and Li,  
M. AdapMoE: Adaptive sensitivity-based expert gating  
and management for efficient moe inference, 2024.